Electronic Supplementary Information

An Efficient Binary Cathode Interlayer for Large-Bandgap Non-Fullerene Organic Solar Cells

Qingwu Yin,[a] Kai Zhang,*[a] Long Zhang,[a] Jianchao Jia,[a] Xi Zhang,[a] Shuting Pang,[a] Zhicheng Hu,[a] Qing-hua Xu, [b] Chunhui Duan,*[a] Fei Huang,*[a] and Yong Cao [a]

[a] Institute of Polymer Optoelectronic Materials and Devices, State Key Laboratory of Luminescent Materials and Devices, South China University of Technology, Guangzhou 510640, P. R. China.

[b] Department of Chemistry, National University of Singapore, 117543, Singapore.

*E-mail: mszhangk@scut.edu.cn; duanchunhui@scut.edu.cn; msfhuang@scut.edu.cn

Experimental Methods

Materials. BDT-ffBX-DT, NT812, SFPDI, PIF-PMIDE-N, PNDIT-F3N, and PIF-PDI-N were synthesized according to the reported procedure. PBDB-T, ITCC and N2200 were purchased from Solarmer Materials Inc. PTB7-Th were purchased from 1-Material Inc. Unless otherwise stated, all reagents and solvents were commonly commercially available products and were used as received.

Fabrication of single and tandem solar cells. The indium tin oxide (ITO) glass substrates were cleaned sequentially under sonication for 30min with acetone, detergent, deionized water and isopropyl alcohol and then dried at 80 °C in baking oven overnight, followed by a plasma treatment for 4 min. The pre-cleaned ITO substrate was coated with PEDOT: PSS (filtered through a 0.22 μm PES filter) by spin-coating (3000 rpm. for 30 s, thickness of ~40 nm) and then baked at 150 °C for 15 min in air. Then, the substrates were transferred into a nitrogen (N_2) protected glovebox. For the single junction device, the active layer BDT-ffBX-DT:SFPDI (weight ration 1:1.5), PBDB-T:ITCC (weight ration 1:1) was prepared in Chlorobenzol solution with 0.5% DIO (v/v), NT812:SFPDI (weight ration 1:1.5) and PTB7-Th:N2200 (weight ration 1:1) was prepared in

Chlorobenzol solution were spin-coated to the optimized thickness according to the reported literatures. The cathode interlayers, PFN-Br, PIF-PMIDE-N, PNDIT-F3N, PIF-PDI-N, or the blend interlayers with different weight ratio dissolved in methanol (with 0.1% acetic acid) at a concentration of 0.5-6 mg/ml were spun onto active layers at 2000 rpm for 30 s for different thickness devices. The thin films were transferred into a vacuum evaporator connected to the glove box, and Ag (100 nm) was deposited sequentially through a shadow mask under ≈10^{-7} Torr, with an active area of the cells of 0.04 cm^2. For the tandem solar cells, the procedure of the front cells was the same as the single-junction except the optimized thickness of front cells was 80nm. A 20nm PIF-PMIDE-N or PIF-PMIDE-N:PNDIT-F3N (4:1) was then spin coated on the active layer. After that, 2nm ultrathin Ag was evaporated onto PIF-PMIDE-N or PIF-PMIDE-N:PNDIT-F3N (4:1) under ≈10^{-7} Torr. Subsequently, 30nm PEDOT: PSS (Clevios PVP AI 4083) was spin coated onto the ultrathin Ag film in ambient atmosphere and then kept in the in a vacuum chamber at a pressure of 10^{-3} Torr to remove the residual water. Then 100-120nm BDT-ffBX-DT:SFPDI active layer was spin coated onto PEDOT:PSS, after that, 5nm PIF-PMIDE-N:PNDIT:F3N (4:1) was spin coated onto BDT-ffBX-DT:SFPDI. Lastly, devices were finished by evaporating 100 nm Ag through a shadow mask in a vacuum chamber with a base pressure of 1 × 10^{-7} Torr. While for the triple junction solar cells, the procedure similar to the tandem solar cells but repeat the twice for the rear sub-cell, and the thickness of active layers was defined to be 70nm, 80nm, and 90nm for the front, medium and rear layer, respectively.

Characterization of device. The current–voltage (*J-V*) curves were measured on a computer-controlled Keithley 2400 source meter under 1 sun, AM 1.5 G spectra from a class solar simulator (Taiwan, Enlitech), the light intensity was 100 mW cm^{-2} as calibrated by a China general

certification center (CGC) certified reference monocrystal silicon cell (Enlitech). Before the *J-V* test, a physical mask of an aperture with precise area of 0.04 cm^2 was used to define the device area. The EQE spectra were performed on a commercial EQE measurement system (Taiwan, Enlitech, QE-R3011). To evaluate the total absorption of the device, the reflection of the device was measured, and the absolute absorption of the devices was calculated by (100-R)%. The reflection was carried out at UV-3600Plus (Shimadzu) with a reflection accessory.

UV-Vis Absorption. UV-vis absorption spectra were measured by using a Hitachi double-beam spectrophotometer UH5300.

UPS measurement. UPS was performed using a standard He-discharge lamp with HeI 21.22 eV as excitation source and an energy resolution of 50 meV. The base pressure of the sample analysis chamber was 5×10^{-9} mbar. All measurements were calibrated by referencing to the Fermi level and Au 4f 7/2 peak position of an Ar^+ ion sputter-clean gold foil.

Electrolysis experiments. The electrolysis experiment was performed on a Labsolar-Ⅲ AG photocatalytic system (PerfectLight) equipment with a reactor containing 60ml NaOH solution (1mg/ml). Platinum wire and platinum sheet was selected to be cathode and anode, respectively. A Xe lamp (300W, Ceaulight) calibrated by AM1.5 filter was used for illumination. The Hydrogen was detected using a gas chromatography (GC7900Ⅱ, USING Ar as carrier gas).

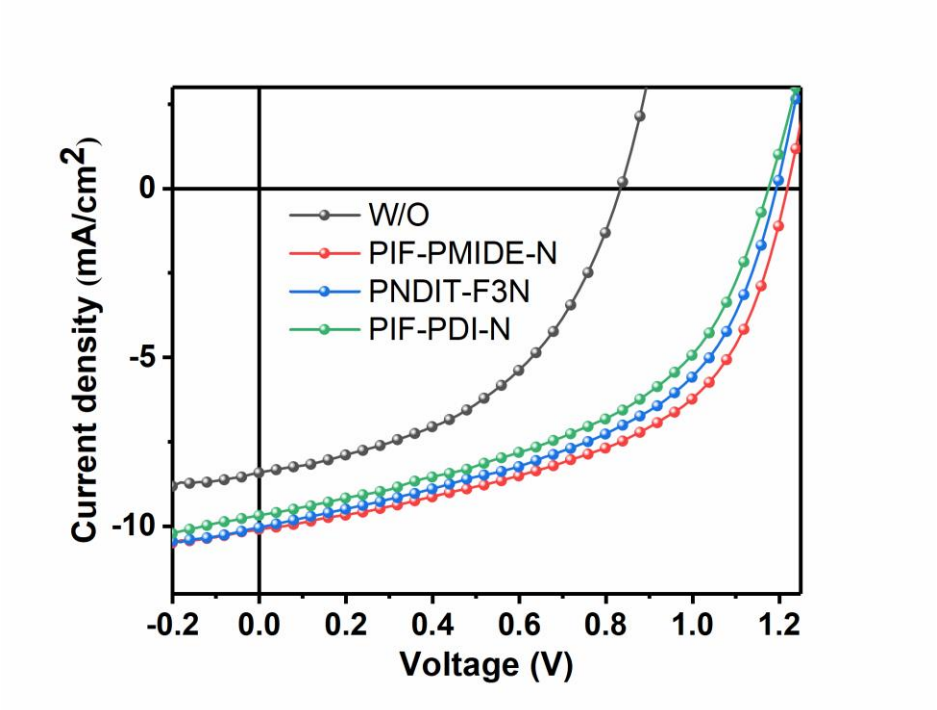

Figure S1 *J*–*V* curves of BDT-ffBX-DT:SFPDI with no and three cathode interlayers.

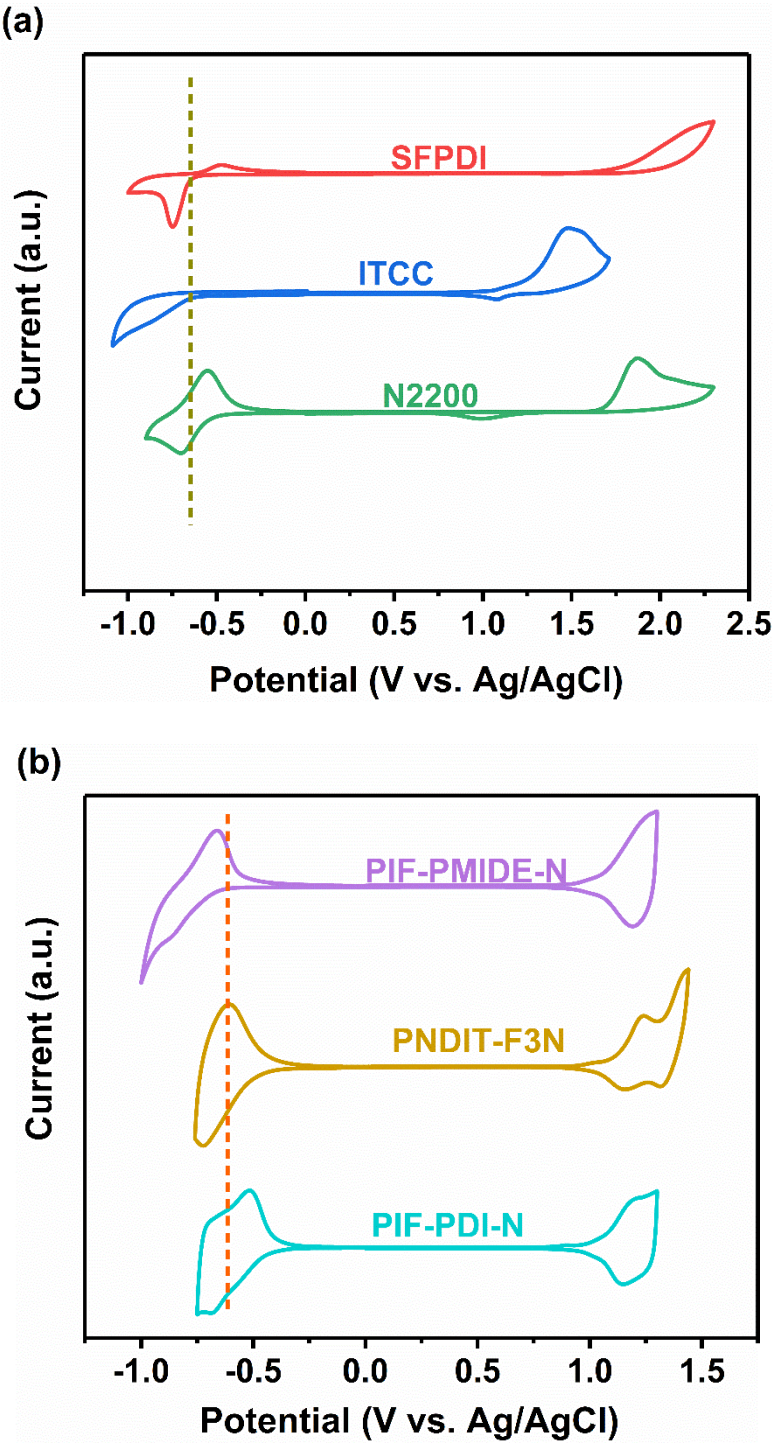

Figure S2 Cyclic voltammograms of acceptors (a) and interlayer materials (b)

Table S1 Electrochemical Properties of the Acceptors and Cathode Interlayers.

		E_{re} (V)	E_{ox} (V)	HOMO[(a)] (eV)	LUMO[(b)] (eV)
Acceptors	SFPDI	-0.66	1.67	-6.0	-3.71
	ITCC	-0.58	1.15	-5.48	-3.75
	N2200	-0.35	1.65	-5.98	-3.98
CILs	PIF-PMIDE-N	-0.65	1.00	-5.33	-3.68
	PNDIT-F3N	-0.44	1.20	-5.53	-3.89
	PIF-PDI-N	-0.41	1.15	-5.48	-3.92

[a] $E_{HOMO} = -(E_{ox}+4.33)$ eV. [b] $E_{LUMO} = -(E_{re}+4.33)$ eV.

Cyclic voltammetry (CV) measurements were used to estimate the frontier molecular orbitals of the copolymers in the thin films. The measurements were carried out under an inert atmosphere by using tetra-n-butylammoniumhexafluorophosphate (n-Bu4NPF6, 0.1M in acetonitrile) as the supporting electrolyte with a glass carbon working electrode, a platinum wire counter electrode, and an Ag/AgCl electrode as the reference electrode. The ferrocene/ferrocenium (Fc/Fc^+) reference was used as an internal standard, which was assigned an absolute energy of −4.8 eV vs vacuum level[1]. Under the same experimental conditions, the onset potential of Fc/Fc^+ was measured to be 0.47 V with respect to the Ag/AgCl reference electrode. On the basis of the onset reduction potential with respect to the standard oxidation potential of the Fc/Fc^+, the lowest unoccupied molecular orbital energy levels (E_{LUMO}) and the highest occupied molecular orbital energy levels (E_{HOMO}) of the copolymers were calculated as $E_{LUMO} = -e(E_{re}+4.33)$ (eV) and $E_{HOMO} = -e(E_{ox}+4.33)$ (eV) respectively[2], where E_{re} (or E_{ox}) is the onset of the reduction (or oxidation) potential vs the Ag/AgCl reference electrode.

Table S2 Experimental device performance of three systems with different interlayers.

D:A	interlayer	V_{oc} (V)	J_{sc} (mA/cm^2)	FF	PCE (%)	Best PCE (%)
NT812:SFPDI	PFN-Br	0.946±0.008	6.39±0.20	0.42±0.01	2.53±0.14	2.58
	PIF-PMIDE-N	0.947±0.001	6.45±0.05	0.42±0.01	2.59±0.04	2.62
	PNDIT-F3N	0.916±0.002	6.24±0.09	0.40±0.01	2.28±0.05	2.33
	PIF-PDI-N	0.864±0.005	6.13±0.06	0.38±0.01	2.03±0.06	2.07
PBDB-T:ITCC	PFN-Br	0.974±0.002	14.88±0.03	0.70±0.01	10.13±0.06	10.2
	PIF-PMIDE-N	0.972±0.003	15.36±0.09	0.66±0.01	9.87±0.14	10.0
	PNDIT-F3N	0.948±0.002	15.22±0.12	0.63±0.01	9.07±0.21	9.20
	PIF-PDI-N	0.932±0.002	15.26±0.15	0.62±0.01	8.84±0.07	8.90
PTB7-Th:N2200	PFN-Br	0.794±0.003	14.41±0.30	0.53±0.01	6.00±0.14	6.16
	PIF-PMIDE-N	0.792±0.001	14.33±0.38	0.53±0.01	5.97±0.14	6.07
	PNDIT-F3N	0.792±0.004	14.22±0.10	0.53±0.01	5.94±0.11	6.02
	PIF-PDI-N	0.790±0.002	14.23±0.41	0.53±0.01	5.97±0.08	6.05

Table S3 Device parameters of single OSCs with binary interlayer contained different ratio of PIF-PMIDE-N:PNDIT-F3N.

ratio	V_{oc} (V)	J_{sc} (mA/cm^2)	FF	PCE (%)	Best PCE (%)
PIF-PMIDE-N	1.218±0.002	10.18±0.27	0.51±0.02	6.31±0.11	6.38
9:1	1.217±0.003	9.99±0.15	0.52±0.02	6.33±0.09	6.39
4:1	1.217±0.003	10.13±0.12	0.52±0.01	6.40±0.02	6.42
3:1	1.212±0.006	9.72±0.25	0.52±0.01	6.10±0.38	6.26
1:3	1.203±0.004	9.71±0.34	0.51±0.02	6.02±0.10	6.09
PNDIT-F3N	1.192±0.005	9.87±0.18	0.49±0.02	5.87±0.09	5.93

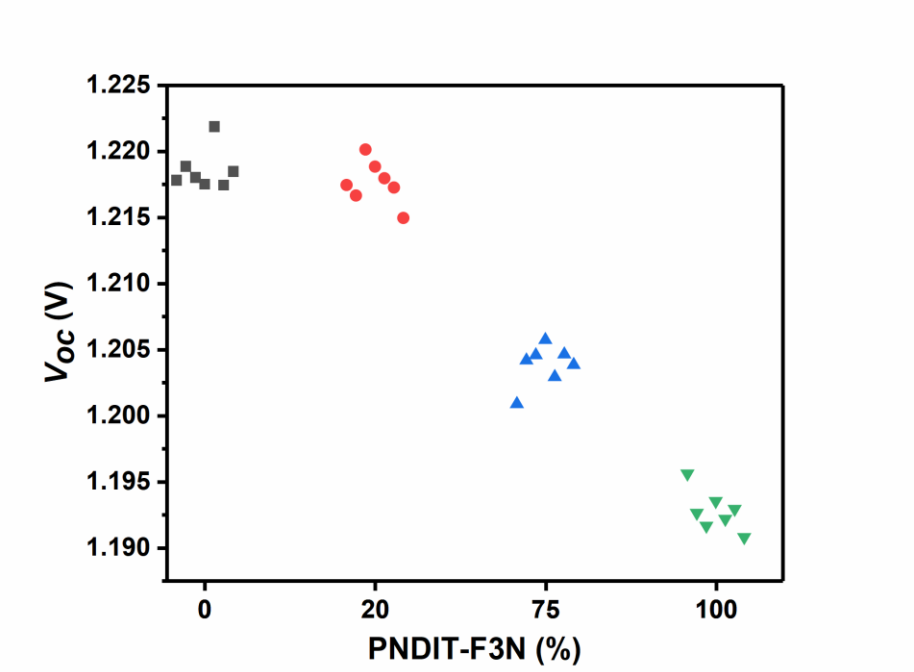

Figure S3 Experimental V_{oc} for binary interlayer contained different ratio of PIF-PMIDE-N:PNDIT-F3N.

Table S4 Summary of results from UPS measurement for blend interlayer films with different ratio.

	Work function (eV)	E_{opt} (eV)	HOMO (eV)	LUMO (eV)
PIF-MIDE-N	3.75	1.72	-5.45	-3.73
9:1	3.74	1.71	-5.47	-3.75
4:1	3.72	1.70	-5.48	-3.78
3:1	3.70	1.69	-5.51	-3.82
1:3	3.68	1.67	-5.53	-3.86
PNDIT-F3N	3.66	1.66	-5.56	-3.90

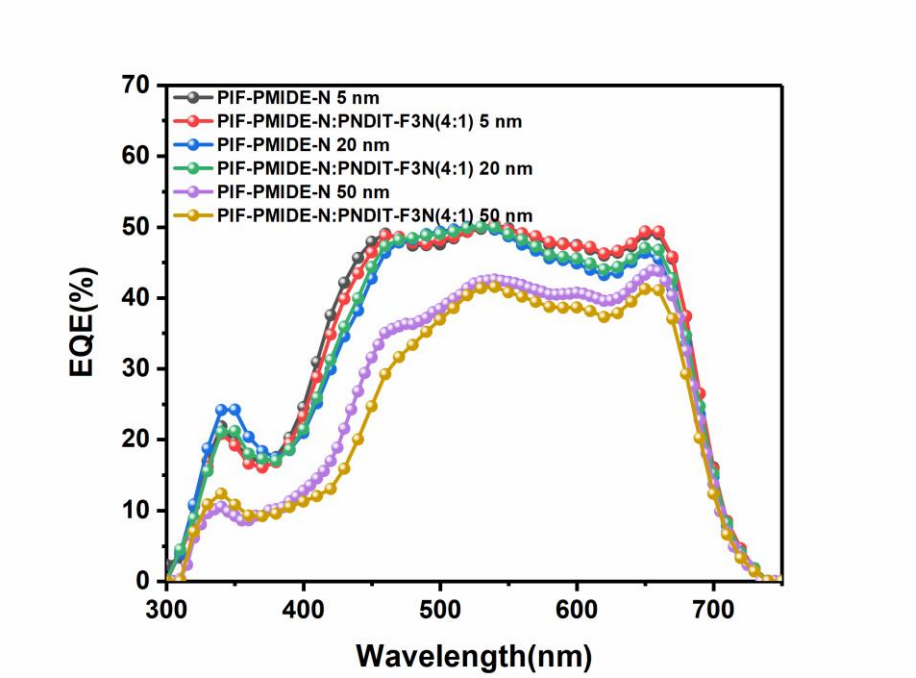

Figure S4 EQE curves of single device based on PIF-PMIDE-N,PIF-PMIDE-N:PNDIT-F3N (4:1) with 5 nm, 20 nm and 50 nm.

Table S5 device date of single junction OSCs with thickness of 80 nm and 110 nm.

	V_{oc} (V)	J_{sc} (mA cm^{-2})	FF (%)	PCE (%)	Best PCE
80 nm	1.21±0.003	8.88±0.18	0.52±0.01	5.65±0.12	5.73
110 nm	1.21±0.001	9.34±0.00	0.53±0.01	6.04±0.02	6.05

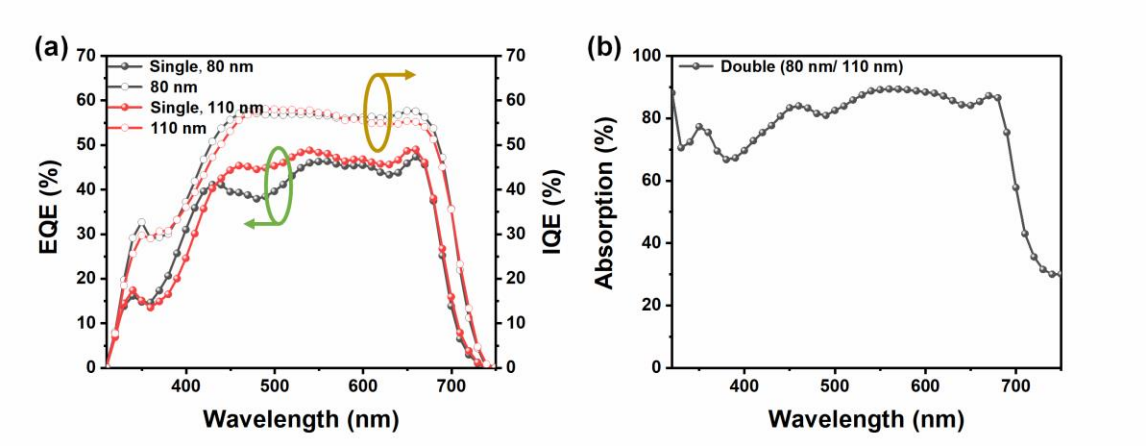

Figure S5 (a) The EQE and IQE of single cells with thickness of 80 and 110 nm, respectively. (b) The total absorption of tandem cell.

The EQE of double junction tandem solar cells can be calculated based on the total absorption of tandem device and IQE of single device. The optimized thickness of front and back cells for double junction tandem OSCs are 80 and 110 nm, respectively. The device performance of single cells with different thickness was shown in table S5, and the EQE and IQE was measured and shown in figure S5(a). The total absorption of double junction tandem OSCs was obtained under the reflection mode (Figure S5(b)). Then the tandem quantum efficiencies (total) can be estimated as maximum and minimum values by multiplying the absorption of the tandem cells with the IQE of the single cells (Figure 4(b)).

^{1}H-NMR and HRMS (MALDI-TOF) of compounds:

PIF-PMIDE-N: **^{1}H NMR** δ_H (500 MHz, $CDCl_3$) 8.74 (1 H, d, *J*=7.6 Hz), 8.62 (1 H, s), 8.36 (1 H, d, *J*=7.8 Hz), 8.33 – 8.25 (2 H, m), 8.22 (1 H, d, *J*=5.8 Hz), 8.08 (1 H, dd, J_1=11.1 Hz, J_2=6.7 Hz), 7.88 – 7.72 (3 H, m), 7.63 (4 H, d, *J*=10.2 Hz), 7.49 – 7.37 (2 H, m), 7.32 (1 H, s), 7.23 (1 H, d, *J*=3.7 Hz), 7.12 (1 H, d, *J*=3.7 Hz), 7.07 (1 H, dd, J_1=8.4 Hz, J_2=3.8 Hz), 4.74 – 4.24 (6 H, m), 4.23 – 3.99 (3 H, m), 2.14 (37 H, t, *J*=82.7 Hz), 1.80 (5 H, ddd, J_1=25.0 Hz, J_2=14.5 Hz , J_3=7.3 Hz), 1.50 (4 H, ddd, J_1=23.4 Hz , J_2=15.5 Hz, J_3=7.7 Hz), 1.39 (12 H, ddd, J_1= 23.1 Hz, J_2=14.9 Hz, J_3=4.9 Hz), 1.14 (11 H, s), 1.05 – 0.79 (13 H, m), 0.75 (7 H, s).

PNDIT-F3N: ^{1}H NMR δ_H (500 MHz, $CDCl_3$) 8.86 (1 H, d, *J*=6.0 Hz), 7.77 (1 H, s), 7.76 – 7.61 (2 H, m), 7.55 (1 H, dd, J_1=17.8 Hz, J_2=6.1 Hz), 7.41 (1 H, d, *J*=3.4Hz), 4.14 (3 H, s), 2.30 (2 H, s), 2.27 – 1.81 (11 H, m), 1.51 – 1.36 (4 H, m), 1.34 (5 H, dd, J_1=12.7 Hz, J_2=6.0 Hz), 0.95 (4 H, t, *J*=7.3 Hz), 0.89 (4 H, dd, J_1=9.3 Hz, J_2=4.7 Hz).

PIF-PDI-N: ^{1}H NMR δ_H (500 MHz, $CDCl_3$) 8.77 (2 H, d, *J*=9.7 Hz), 8.48 (2 H, t, *J*=11.8 Hz), 8.35 (2 H, d, *J*=8.1 Hz), 7.78 (2 H, s), 7.64 (5 H, d, *J*=5.3 Hz), 7.46 (2 H, s), 7.35 (2 H, s), 7.16 (1 H, d, *J*=8.2 Hz), 4.14 (4 H, s), 2.61 – 1.61 (41 H, m), 1.59 – 0.98 (34 H, m), 0.97 – 0.38 (19 H, m).

SFPDI: ^{1}H NMR δ_H (500 MHz, $CDCl_3$) δ 8.52-8.59 (10H, m), 8.09-8.21 (4H, m), 7.44-7.82 (6H, m), 7.04 – 7.16 (4H, m), 6.75-6.90 (4H, m), 5.23 – 5.11 (4H, m), 2.23-2.25 (8H, m), 1.83 (8H, s), 1.25

(48H, s), 0.83 (24H, s). **MS (MALDI-TOF):** Calc. for $C_{117}H_{120}N_4O_8$: 1708.91. Found: 1731.42[M+Na+].

ITCC: ^{1}H NMR δ_H (500 MHz, $CDCl_3$) 8.13 (1 H, s), 7.93 (2 H, q, *J*=4.9 Hz), 7.62 (1 H, s), 7.20 (4 H, d, *J*=8.4 Hz), 7.13 (4 H, d, *J*=8.4 Hz), 2.64 – 2.49 (4 H, m), 1.58 (4 H, dd, J_1=15.5 Hz, J_2=7.8 Hz), 1.41 – 1.18 (12 H, m), 0.86 (6 H, t, *J*=6.8 Hz). **MS (MALDI-TOF):** Calc. for $C_{90}H_{78}N_4O_2S_6$: 1438.44. Found: 1439.08[M+].

N2200: ^{1}H NMR δ_H (500 MHz, $C_2D_2Cl_4$) 8.87 (1 H, s), 8.62 (3 H, s), 7.41 (3 H, s), 4.16 (2 H, s), 2.05 (4 H, s), 1.67 (14 H, s), 1.32 (60 H, s), 0.91 (15 H, s).

BDT-ffBX-DT: ^{1}H NMR δ_H (400 MHz, $C_2D_2Cl_4$, 100℃) 7.57 (1 H, s), 3.01 (1 H, s), 1.55 (18 H, dd, J_1=114.7 Hz, J_2=46.2 Hz), 0.95 (3 H, s).

NT812: ^{1}H NMR δ_H (400 MHz, $oC_6D_4Cl_2$,100℃) 8.23 (1 H, s), 7.42 (1 H, d, *J*=44.4 Hz), 3.02 (1 H, s), 1.39 (25 H, d, *J*=118.9 Hz), 0.82 (4 H, s).

PBDB-T: ^{1}H NMR δH (400 MHz, $C_2D_2Cl_4$, 100℃) 7.83 (1 H, s), 7.39 (2 H, d, *J*=25.8 Hz), 7.02 (2 H, s), 3.42 (2 H, s), 2.99 (2 H, s), 1.85 (3 H, s), 1.00 (42 H, d, *J*=38.8 Hz).

PTB7-Th: ^{1}H NMR δ_H (400 MHz, $C_2D_2Cl_4$, 100℃) 8.28 – 7.66 (1 H, m), 7.50 (1 H, d, J 46.9), 7.03 (1 H, s), 4.36 (1 H, s), 3.00 (2 H, s), 1.87 (2 H, s), 1.48 (17 H, s), 1.07 (10 H, t, *J*=28.2 Hz).

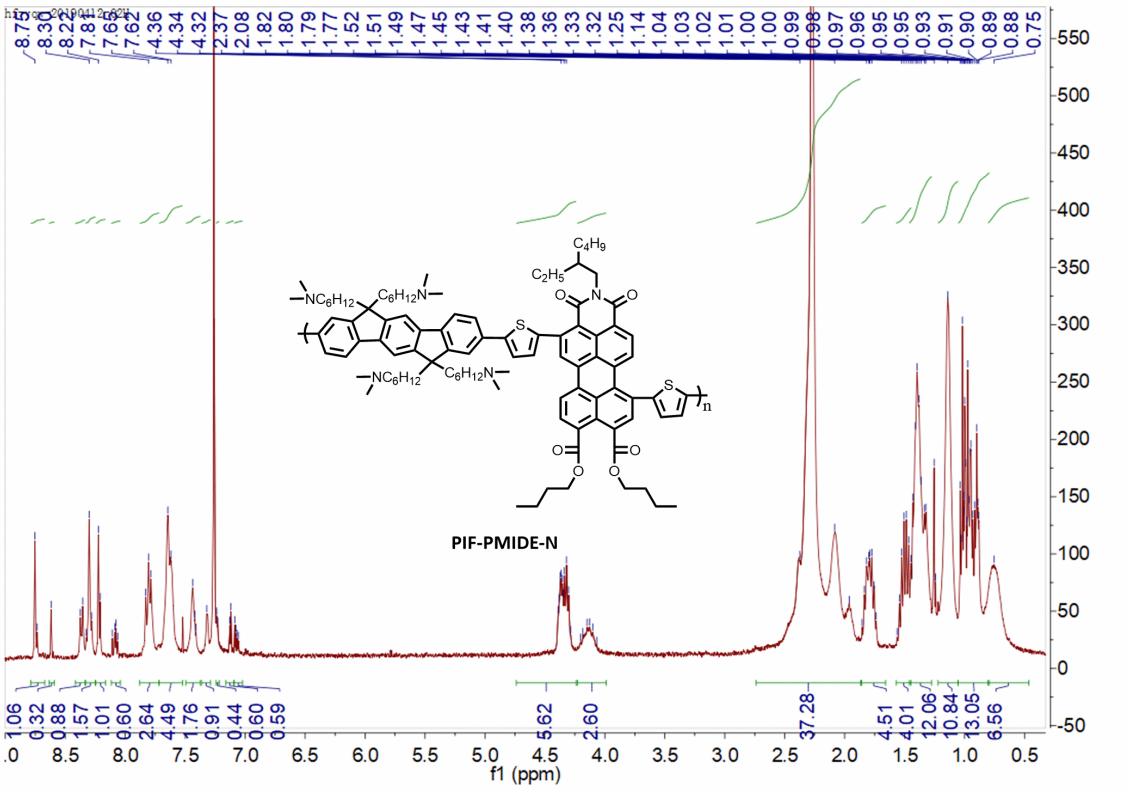

Figure S6 ^{1}H NMR spectrum of PIF-PMIDE-N.

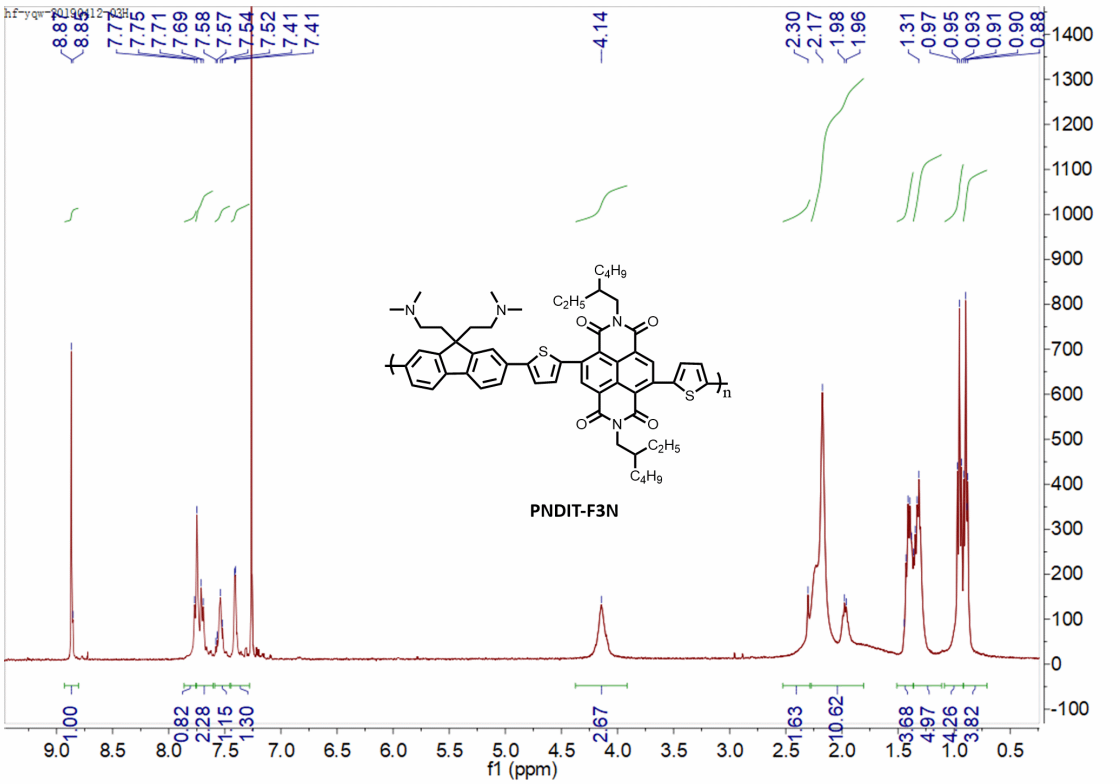

Figure S7 ^{1}H NMR spectrum of PNDIT-F3N.

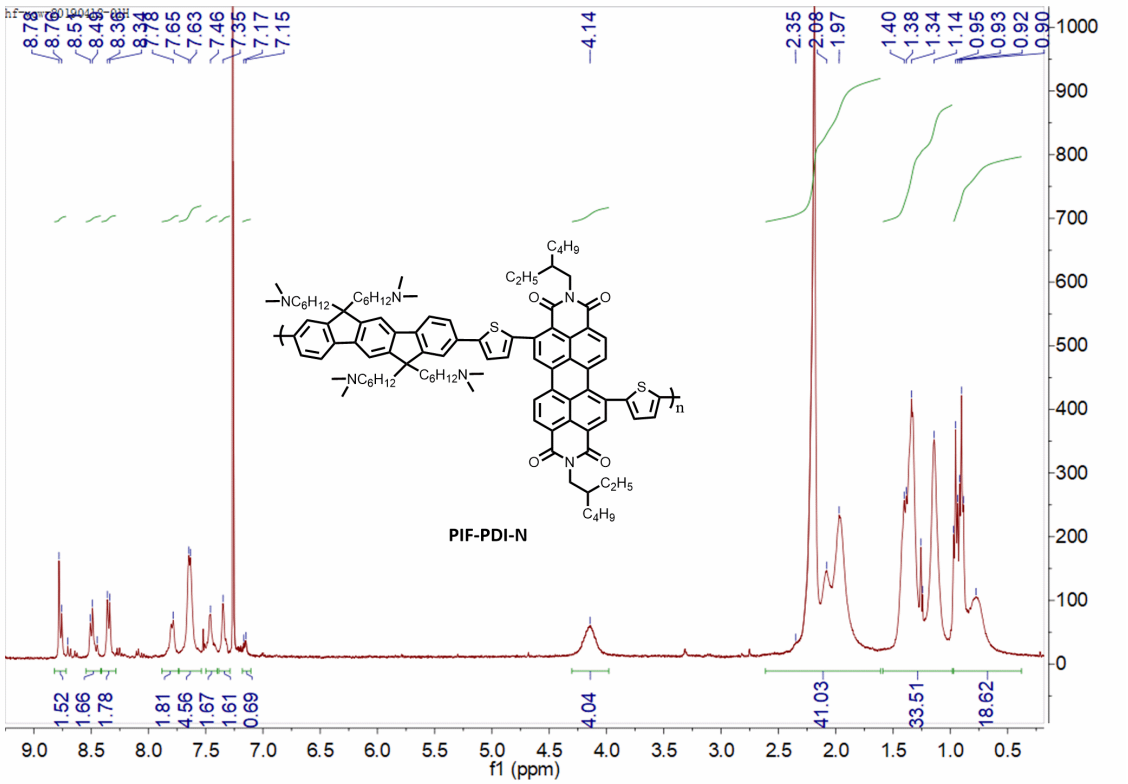

Figure S8 ^{1}H NMR spectrum of PIF-PDI-N.

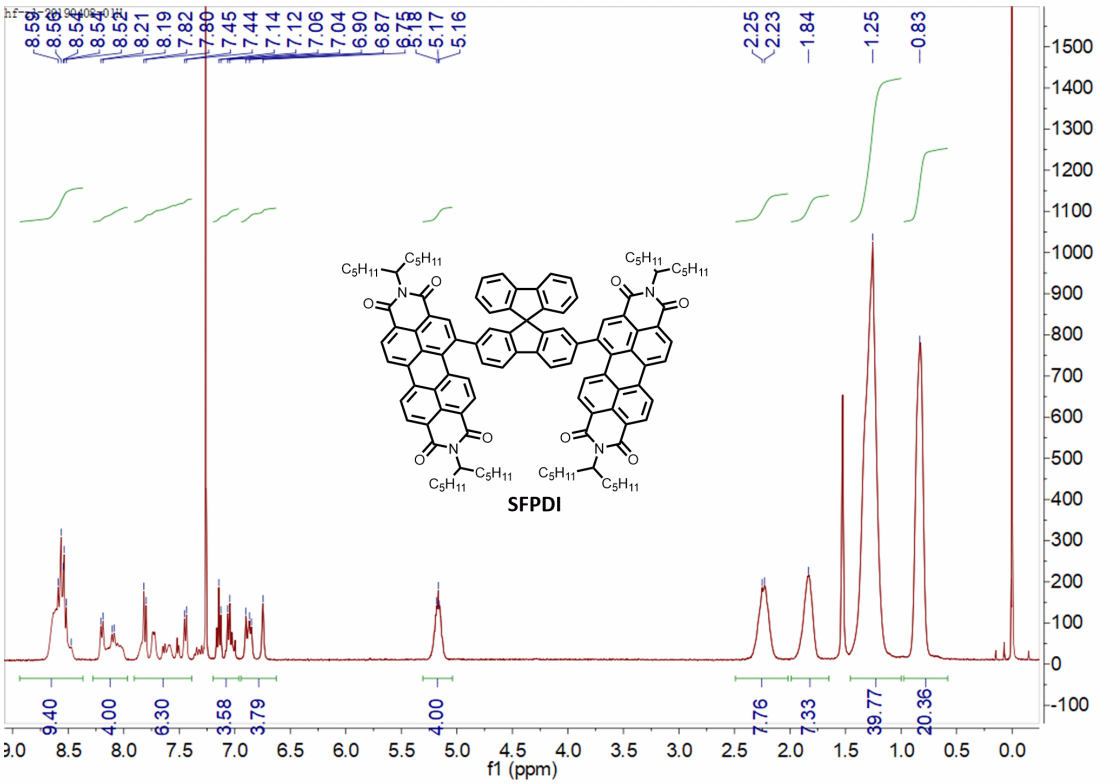

Figure S9 ^{1}H NMR spectrum of SFPDI.

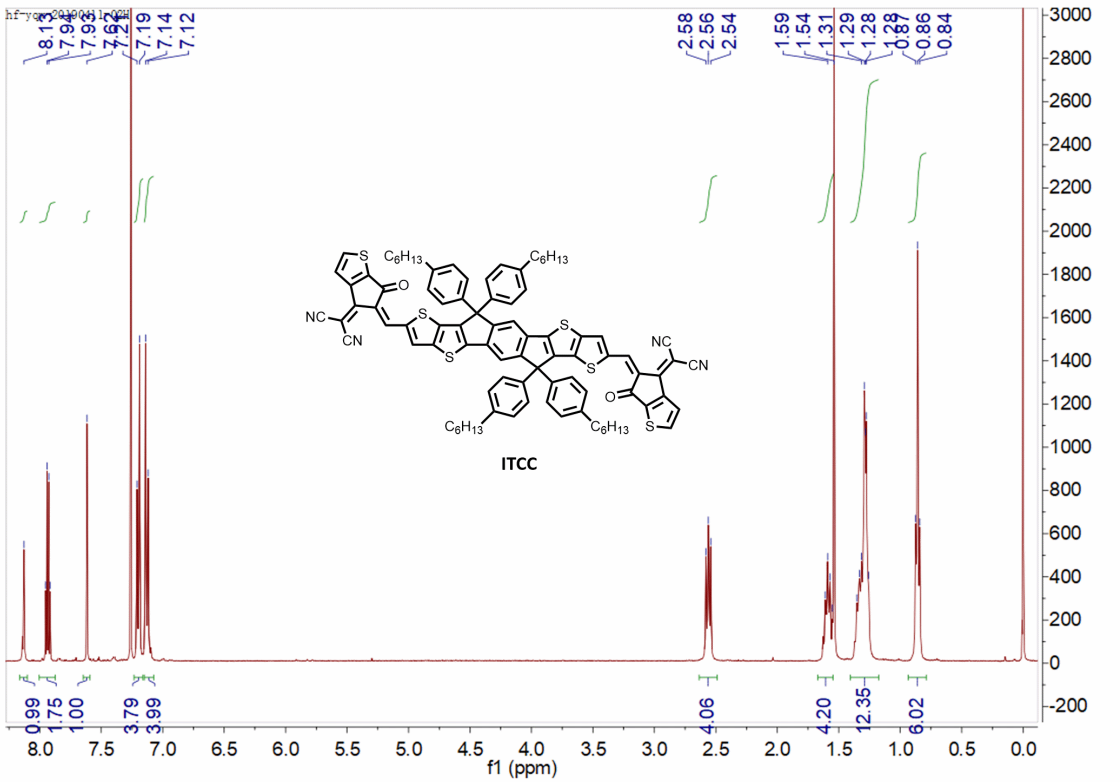

Figure S10 ^{1}H NMR spectrum of ITCC.

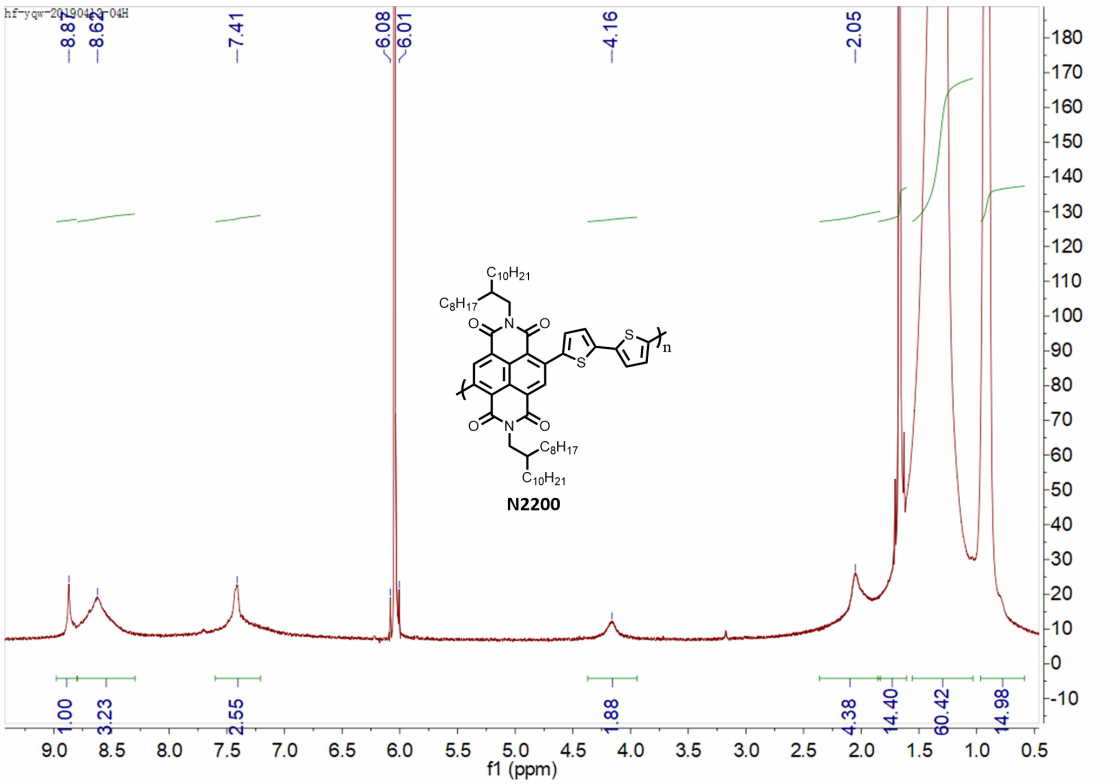

Figure S11 ^{1}H NMR spectrum of N2200.

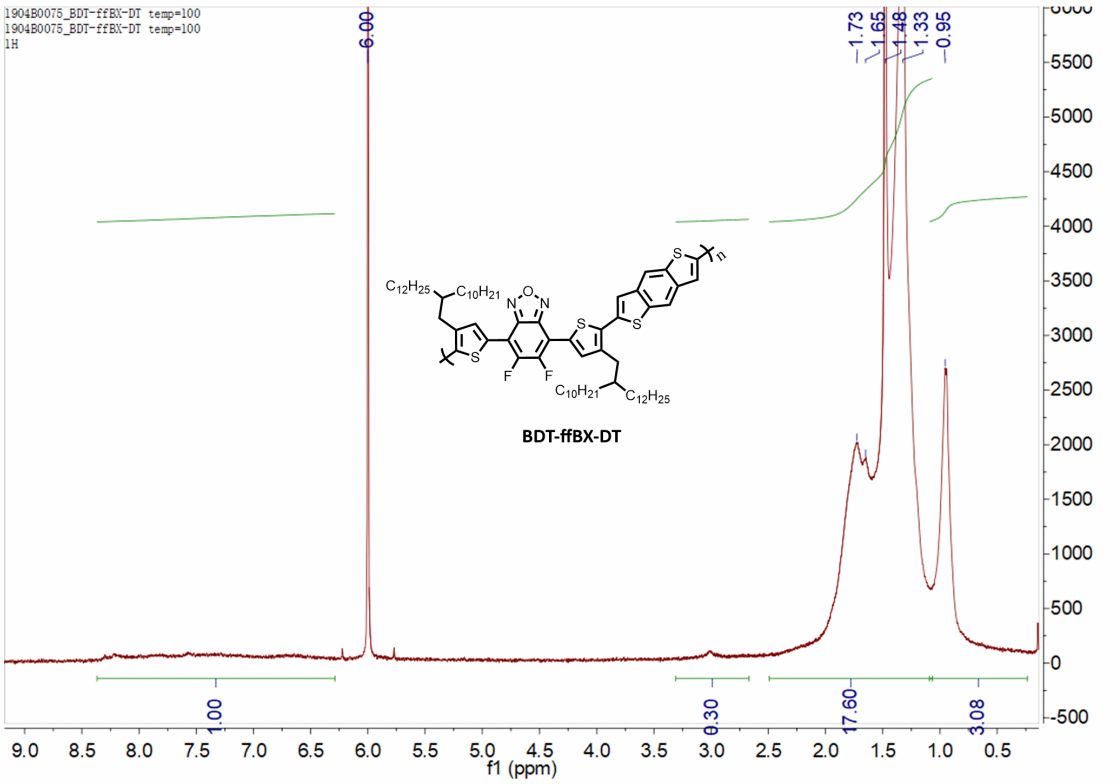

Figure S12 ^{1}H NMR spectrum of BDT-ffBX-DT.

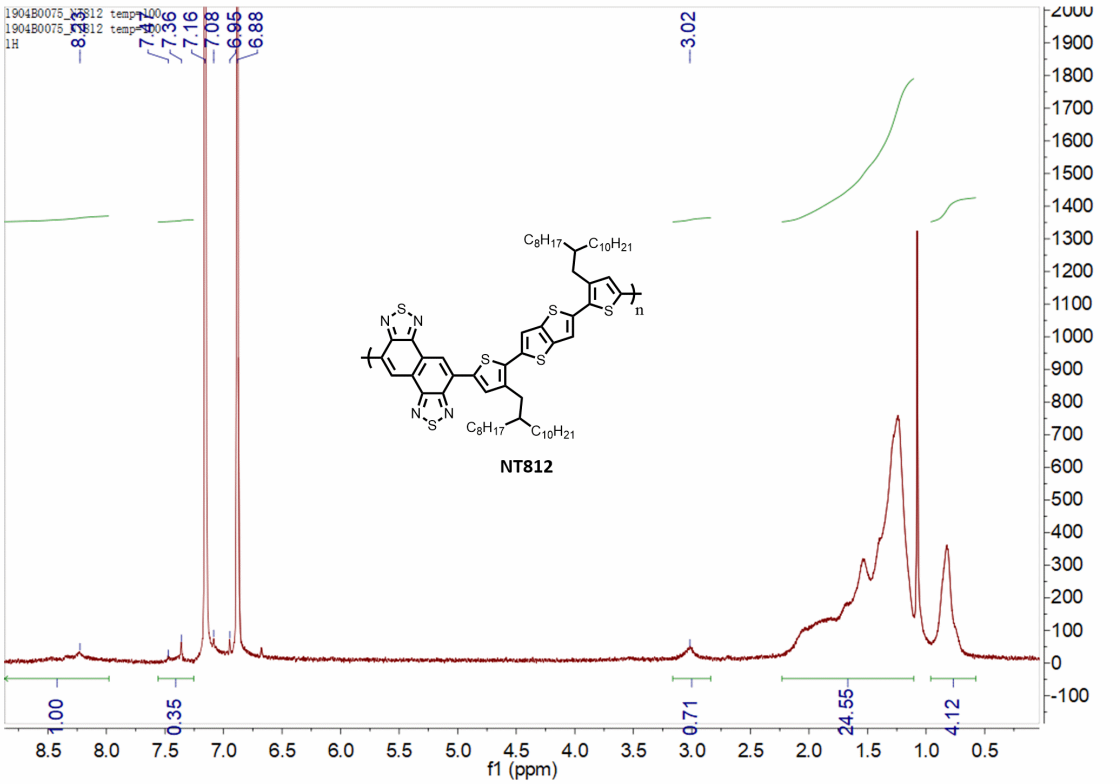

Figure S13 ^{1}H NMR spectrum of NT812.

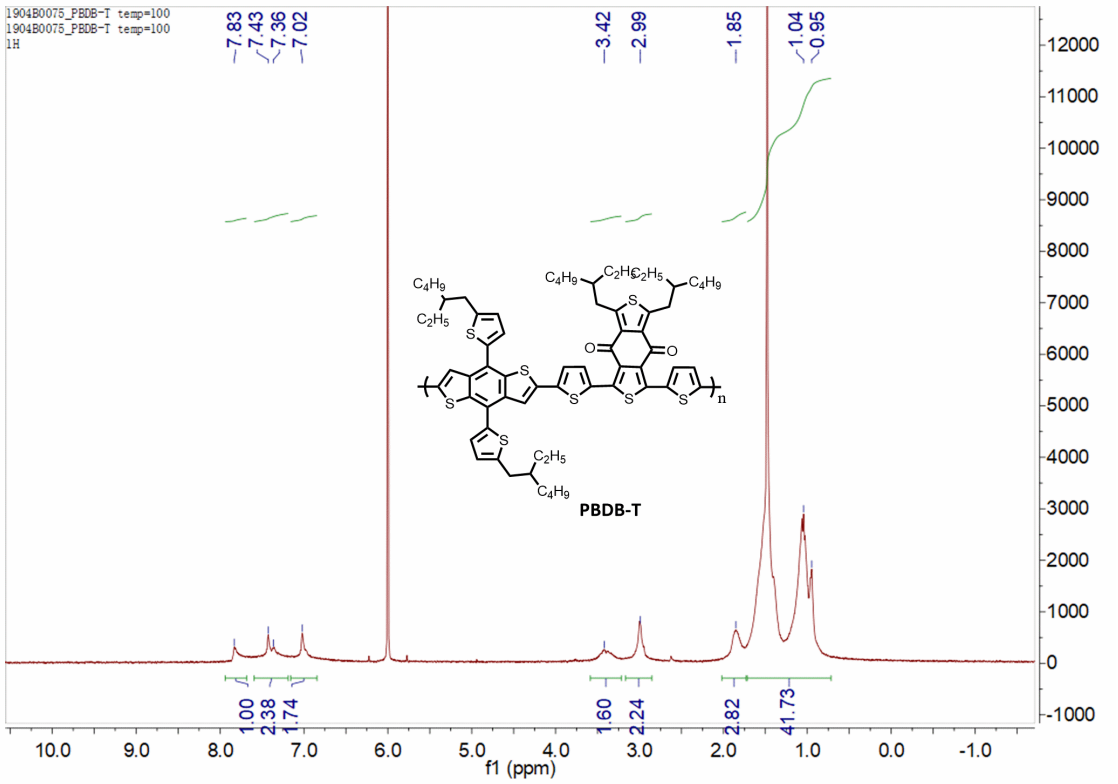

Figure S14 ^{1}H NMR spectrum of PBDB-T.

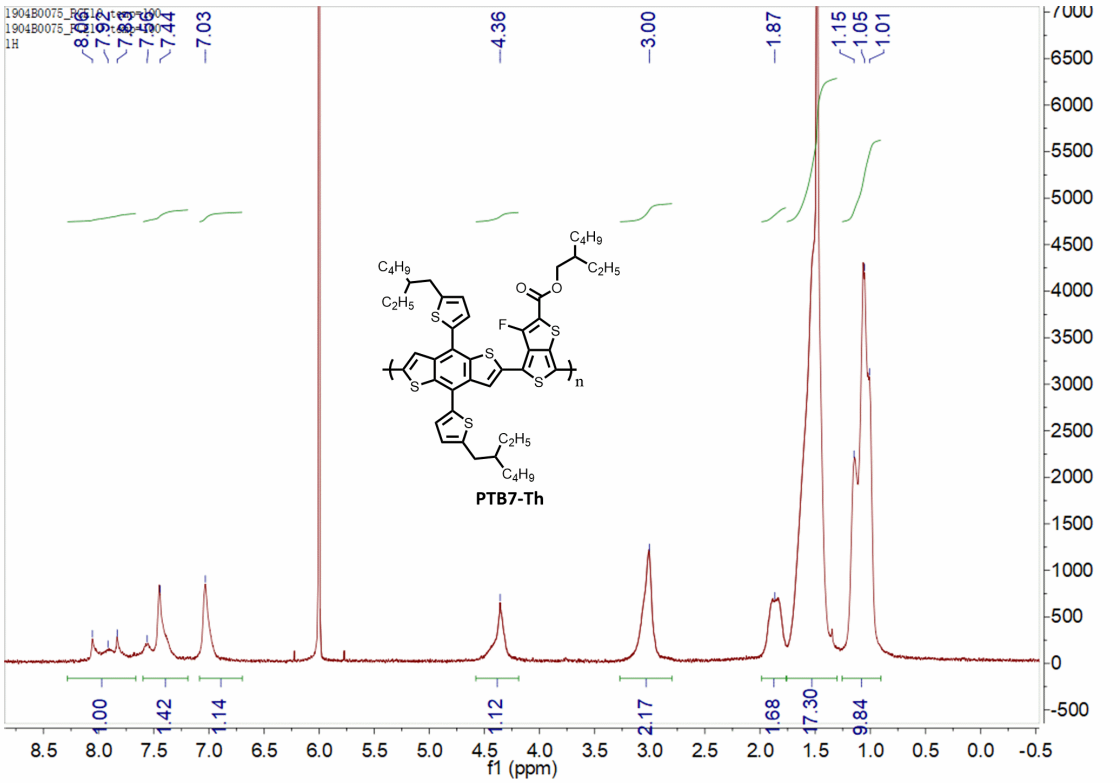

Figure S15 ^{1}H NMR spectrum of PTB7-Th.

1. V. V. Pavlishchuk and A. W. Addison, *Inorganica Chimica Acta*, 2000, **298**, 97-102.
2. Y. Li, Y. Cao, J. Gao, D. Wang, G. Yu and A. J. Heeger, *Synthetic Metals*, 1999, **99**, 243-248.